Biosensors and Bioelectronics 77 (2016) 1201–1207

Contents lists available at ScienceDirect

Biosensors and Bioelectronics

journal homepage: www.elsevier.com/locate/bios

Use of liposomal amplifiers in total internal reflection fluorescence fiber-optic biosensors for protein detection

Ying-Feng Chang [a,1], Chen Fu [b,1], Yi-Ting Chen [b,1], Amily Fang-Ju Jou [a], Chii-Chang Chen [c], Chien Chou [d,e], Ja-an Annie Ho [a,b,*]

[a] BioAnalytical Chemistry and Nanobiomedicine Laboratory, Department of Biochemical Science and Technology, National Taiwan University, Taipei 10617, Taiwan
[b] Department of Chemistry, National Tsing Hua University, Hsinchu 30013, Taiwan
[c] Department of Optics and Photonics, National Central University, Taoyuan 32001, Taiwan
[d] Graduate Institute of Electro-Optical Engineering, Chang Gung University, Taoyuan 33302, Taiwan
[e] Healthy Aging Research Center, Chang Gung University, Taoyuan 33302, Taiwan

ARTICLE INFO

Article history:
Received 1 July 2015
Received in revised form
2 October 2015
Accepted 4 October 2015
Available online 8 October 2015

Keywords:
Liposomes
Protein detection
Evanescent wave-excited fluorescence
Fiber-optic biosensors

ABSTRACT

Evanescent-wave excited fluorescence technology has been demonstrated to enhance sensitivity and reduce matrix effects, making it suitable for biosensor development. In this study, we developed a liposome-based, total internal reflection fluorescence, fiber-optic biosensor (TIRF-FOB) for protein detection, which integrates a liposomal amplifier and sandwich immunoassay format with TIRF-FOB. In addition, the antibody-tagged and fluorophore-entrapped liposomes for heterogeneous detection of target molecules were designed and synthesized. This biosensor successfully detected the target protein (model analyzed here is IgG) with a limit of detection (LOD) of 2.0 attomoles for the target protein (equivalent to 2.0 pg/mL of protein presented in 150 μL of sample solution). The features of this ultrasensitive liposomal TIRF-FOB are (i) fluorescence is excited via evanescent waves and amplified via liposomes; (ii) the use of two polyclonal antibodies in the sandwich assay format increases the specificity and lowers the cost of our assay. Based on the exceptional detection sensitivity and cost-effectiveness, we believe that the proposed biosensor has great potential as a practical, clinical diagnostic tool in the near future.

1. Introduction

Optical fibers were used commonly as a means to allow light propagation with the least loss, and they were found to have a use in sensor development during the 1960s (Marazuela and Moreno-Bondi, 2002). Fiber-optic biosensors (FOB), which use optical fiber as the transduction element and which rely mostly on evanescent-sensing for detecting target biomolecules, have been employed widely in diagnostic fields (Queiros et al., 2014; Wang et al., 2015; Wang and Wolfbeis, 2013). To achieve evanescent-sensing, the cladding of the optical fiber must be removed, which enables the evanescent field that is excited by the total internal reflection of transmitted light to interact with the surroundings (Leung et al., 2007). The response readouts acquired by FOB are often based on changes in one specific optical property (i.e., light intensity, phase, resonance wavelength) attributed to the interaction of the recognition element with its target. In 1975, Kronick and Little first reported total internal reflection fluorescence (TIRF) technology for detecting antibody-antigen binding (Kronick and Little, 1975); since then, TIRF technology becomes one of the most frequently used and effective techniques combined with FOB, because it not only can enhance sensitivity but also improve discrimination for specific binding from non-specific adsorption of target analytes. The foremost feature of TIRF-FOBs is to detect biomolecules-of-interest located on or near the outer surface of the uniformly declad optical fiber, thereby providing a way to directly evaluate ligand–receptor interactions occurring at the surface–solution interface (Marazuela and Moreno-Bondi, 2002). In addition, the capabilities of TIRF-FOBs include (i) cost effectiveness, (ii) chemical-inertness, (iii) well-established strategies for surface modifications, (iv) practicability for remote sensing and, finally, (v) accessibility of reasonably priced photodetectors (Leung et al., 2007). However, the sensitivity provided by conventional TIRF-FOBs that were not further coupled with other fluorescence-enhanced technique (Hao et al., 2014; Liu et al., 2015b) may still not be as satisfactory as other methods, such as enzyme-linked

* Corresponding author at: BioAnalytical Chemistry and Nanobiomedicine Laboratory, Department of Biochemical Science and Technology, National Taiwan University, Taipei 10617, Taiwan. Fax: +886 2 33662271.
E-mail address: jaho@ntu.edu.tw (J.-a. Annie Ho).
[1] These three authors contributed equally to this work.

http://dx.doi.org/10.1016/j.bios.2015.10.012
0956-5663/

immunosorbent assay (ELISA) (Zhang et al., 2014) and electrochemical method (Liu et al., 2015a). To improve its detection sensitivity, several advanced fluorescence-enhanced techniques may be integrated with TIRF-FOB, such as photonic crystal-enhanced fluorescence (Chaudhery et al., 2013; Pokhriyal et al., 2010), graphene oxide-enhanced fluorescence (Geng et al., 2013; Yu et al., 2013), metal-enhanced fluorescence (Chang et al., 2014a, 2014b, 2015, 2013; Chao et al., 2012), and liposomal fluorescence amplifier (Ho et al., 2004, 2006, 2007, 2008; Ho and Hung, 2008; Vamvakaki et al., 2005); thus far, only the metal-enhanced fluorescence technique has been demonstrated to detect protein–protein interactions (Chang et al., 2009, 2011, 2010; Hsieh et al., 2007; Huang et al., 2009; Su et al., 2011). Although the detection limits of such FOBs have been improved to the pg/mL level, the possible causes of irreproducible performance remain uncertain (Chang et al., 2013). Therefore, we attempted to assimilate TIRF-FOB with a liposomal fluorescence amplifier to demonstrate the feasibility of a new biosensing platform.

Liposomes were discovered almost 50 years ago by Bangham's group (Bangham et al., 1965) and they have since become highly versatile tools for use in biology, biochemistry, and medicine (Chandrasekaran and King, 2014; Ho et al., 2004; Niehage et al., 2014; Noble et al., 2014; Patil and Jadhav, 2014). Liposomes are nanoscale, spherical vesicles composed of natural, nontoxic phospholipids and cholesterol and are similar in almost every aspect to small cells (Ho et al., 2004). Liposomes are produced easily and they are stable in solution for long periods of time without significant changes occurring in size or structure (Vamvakaki et al., 2005; Woodle. 1995). Moreover, their ability to carry different molecules in their aqueous cavity make them very appealing for a wide range of applications, such as clinical diagnostics, drug delivery, and gene therapy (Fan et al., 2012; Ho et al., 2012, 2004; Vamvakaki et al., 2005).

Liposomes may also function as signal amplifiers. Signal amplification of the binding event between the target analyte and its structurally complementary counterpart is the principal concern in the development of biosensing devices. Although enzyme amplification is one of the most commonly used signal amplification systems in immunoassays, an incubation time is required for substrate turnover (Ho et al., 2004). In contrast, liposomes—that encapsulate detectable molecules such as dyes and other markers—provide instantaneous rather than time-dependent enhancement that normally limits the speed of analysis and the sensitivity of enzyme immunoassays. Fluorochromes such as sulforhodamine B (SRB) and carboxyfluorescein (CF) are common markers used in liposome immunoassays that can be quantitatively determined by spectrophotometers or perceived by the naked eye.

In this study, a liposome-based TIRF-FOB for protein detection was proposed and developed, which unites liposome-based fluorescence signal amplifiers, sandwich immunoassay, and TIRF-FOB. The resulting biosensor demonstrated unique features, where fluorescence was excited via evanescent waves and amplified via antibody-tagged, fluorescent molecules-entrapped liposomes. In addition, the liposome-based TIRF-FOB not only showed a high sensitivity and specificity for detection, but it also required fewer expensive reagents, which is integral to manufacturing a cost-effective sandwich immunoassay.

2. Materials and methods

2.1. Materials

Goat anti-mouse IgG antibody (used as both the capture antibody and the detection antibody), mouse IgG (used as the target protein), FITC-labeled antibody, bovine serum albumin (BSA), chloroform, cholesterol, ethylenediaminetetraacetic acid (EDTA), N-ethylmaleimide (NEM), 4-(2-hydroxyethyl)-1-piperazineethanesulfonic acid (HEPES), isopropyl ether (IPE), methanol (MeOH), 5(6)-carboxyfluorescein (CF), ethyl acetate (EA), glutaraldehyde (GA), isopropanol (IPA), poly(ethyleneimine) (PEI), Triton X-100, and phosphate buffered saline (PBS) were purchased from Sigma (St. Louis, MO, USA). Hydroxylamine hydrochloride was obtained from Fluka (St. Louis, MO, USA). Dipalmitoylphosphatidylcholine (DPPC), dipalmitoylphosphatidylglycerol (DPPG), and dipalmitoylphosphatidylamine-N-[4-(p-maleimidomethyl) cyclohexane-carboxamide] (PEMCC) were obtained from Avanti Polar Lipids (Alabaster, AL, USA). N-succinimidyl-S-acetylthioacetate (SATA) was purchased from Invitrogen (Carlsbad, CA, USA). The plastic optical fibers (diameter: 1 mm) and dialysis bag (MWCO:12–14 kDa) were purchased from Mitsubishi Rayon Co., Ltd. (Tokyo, Japan) and Spectrum Laboratories Inc. (Rancho Dominguez, CA, USA), respectively.

2.2. Preparation of liposomes

Liposomes were prepared by a reversed-phase evaporation method based on a water-in-oil emulsion strategy (Ho and Hsu, 2003; Ho and Hung, 2008). The lipid mixture consisted of DPPC, cholesterol, DPPG, and PEMCC (in a molar ratio of 10:10:1:0.2); the lipid mixture was first dissolved in a solvent mixture consisting of chloroform and methanol (8:2), followed by 1 min sonication at 45 °C under nitrogen. One milliliter of 10 mM CF was then added to the lipid mixture under continuous sonication to generate an emulsion. After sonication of the solution for a further 3 min with occasional swirling, the organic solvent was removed by rotary evaporation at 45 °C, leaving an orange, gel-like suspension of liposomes. Finally, an additional aliquot of CF was added, followed by another 3 min of sonication at 45 °C. The liposome preparation was then incubated in a 45 °C water bath for 30 min before passing through 0.2 μm and 0.4 μm polycarbonate filters to produce a homogenous suspension with a uniform size of liposomes. Any unencapsulated CF dye or trace of organic solvent was removed from the liposome preparation by gel filtering on a Sephadex G-75–50 column at ambient temperature.

2.3. Preparation of SATA-modified antibodies

Immediately before reaction, a 0.558 μmol sample of SATA in DMSO (20 μL) was added to the 80 μL detection antibody solution (1 mg/mL in 10 mM PBS solution at pH 7.6), and the mixture was allowed to react for 90 min at room temperature in the dark. Deacetylation of the SATA-modified protein was carried out by adding 0.5 M hydroxylamine hydrochloride solution (pH 7.5) to the mixture, followed by incubating the reaction mixture for 2 h at room temperature. Finally, a Sephadex G-25 gel filtration column was used to purify the sulfhydryl-modified antibody from the hydroxylamine.

2.4. Conjugation of maleimide-derivatized liposomes with SH-containing detection antibody

The coupling of maleimide-reactive detection antibodies with the thiol-reactive liposomes was achieved by incubating two reaction solutions for 2 h at room temperature, followed by an overnight reaction at 4 °C. A 1.116 μmol sample of N-ethylmaleimide was introduced into the mixture to interact with the unreacted SATAs. At last, the antibody-tagged and fluorophore-entrapped liposomes, named as liposomal amplifiers in this study, were purified by dialysis (MWCO: 12–14 kDa) against a 10 mM PBS buffer.

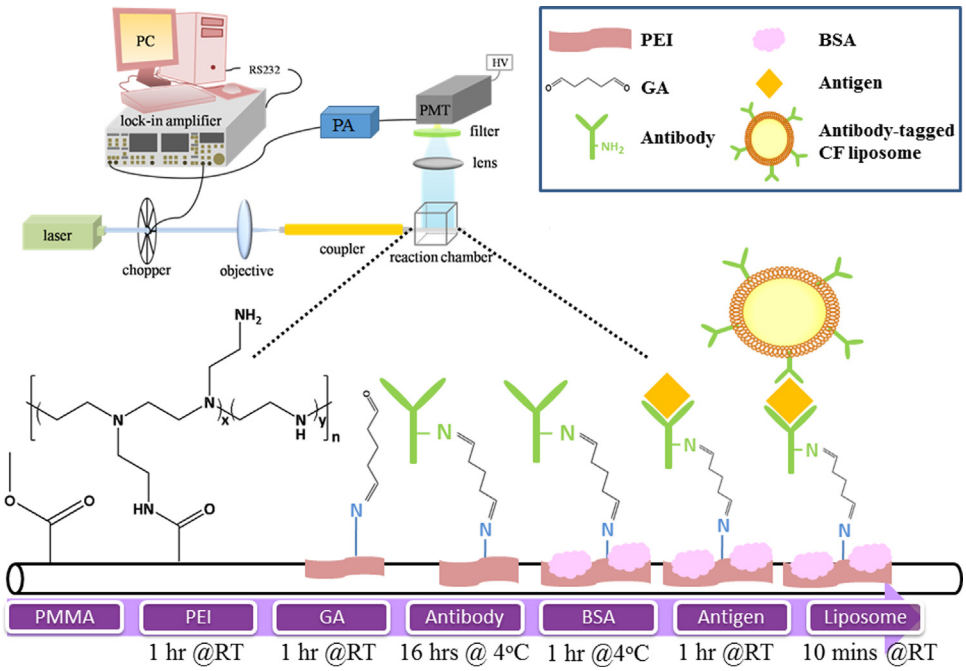

Fig. 1. Schematic diagram of chemical modification to the optical fibers and the optical setup of our TIRF-FOB.system.

2.5. Surface modification of plastic fibers and optimization study

Cladding of the plastic optical fibers was stripped off first by immersion in EA. The stripped portion was cleaned subsequently with IPA, generating a clean, stripped area of 46 mm^2. A chemical adsorption method that introduces functional amine groups on the plastic surface was adopted to immobilize the capture antibody on the surface of the de-cladded portion via covalent binding forces. Schematic diagram of chemical modification to the optical fiber is illustrated in Fig 1. In short, the portion was modified via immersion in PEI solution (pH 11.5) at room temperature for 1 h. Subsequently, the modified portion was incubated with 1% GA at room temperature for an additional 1 h. The PEI-GA modified portion of optical fiber was then immersed in 150 µL of capture antibody (10 µg/mL) at 4 °C for 16 h. After blocking with 10 mg/mL BSA in PBS solution for 1 h, the fibers were ready to measure the target protein, mouse IgG. The optimum PEI concentration used for surface-modifying optical fiber and optimum pH selected for subsequent derivatization with GA were also investigated.

2.6. Optical setup for TIRF-FOB and assay procedure using the liposomal amplifiers

The optical setup of the liposome-based TIRF-FOB is illustrated in Fig. 1. A 488 nm sapphire laser (20 mW, Coherent, Santa Clara, CA, USA) was used as the excitation light source, and the pumped intensity of laser beam was modulated mechanically with a chopper frequency of 1 kHz. A microscope objective (10 ×; numerical aperture = 0.27) was used to achieve the best coupling efficiency. As a result, an intensity-modulated evanescent wave was generated in the modified portion of the fiber surface that was able to excite the trapped CF fluorophores inside the liposomal amplifiers. The emitted fluorescence was collected in the geometry that was normal to the reaction chamber to avoid the laser beam-induced background. The CF fluorophores contained in the liposome amplifiers have strong absorption at 492 nm and high fluorescence emission at 517 nm, thus a long pass filter (cutoff wavelength ~500 nm) was introduced into our setup to allow fluorescence detection by a photomultiplier tube (Hamamatsu, Shizuoka, Japan), and a lock-in amplifier (Stanford Research Systems, Sunnyvale, CA, USA) was used to detect experimentally the intensity-modulated fluorescence signal.

The as-prepared optical fiber that had been coated with capture antibody and blocked with BSA was installed in the TIRF-FOB. 150 µL aliquots of serially diluted IgG in PBS solutions were added to each individual reaction chamber and incubated at room temperature for 1 h to form the < capture antibody/target protein > complexes on the modified fiber surface. The fibers were then washed at least 5 times with PBS solution to remove unbound target protein. Finally, 150 µL of liposomal amplifier solution was added to each reaction chamber, and the < capture antibody/target protein/liposomal amplifier > sandwich immunocomplexes were formed subsequently (as shown in Fig. 1). The fluorescence attributed to the bound liposomal amplifiers was then measured quantitatively by the TIRF-FOB.

2.7. Data analysis

All fitting curves were analyzed with GraphPad Prism software to fit a nonlinear regression using a four-parameter dose-response curve (variable slope model), which is defined by:

$$Y = B + \frac{A - B}{1 + 10^{((\log C - X) \times D)}}$$

Where Y is the signal output, X is the analyte concentration, A is the highest signal, B is the lowest signal, C is the concentration corresponding to the half-maximal signal, and D describes the steepness of the calibration curve. According to the International Union of Pure and Applied Chemistry (IUPAC), the operational definition of detection limit in this study was calculated at the concentration corresponding to a signal 3 SD (standard deviation) above the mean for a calibrator that is free of target analyte.

3. Results and discussion

3.1. Characteristics of liposomes

For our particular optical sensing, the size of liposomes must be smaller than the penetration depth of the evanescent wave (around 475 nm), and the optimum concentration of CF inside the liposomes (10 mM) was selected to avoid self-quenching (Lakowicz et al., 2003). Because the final signal output was attributed to the fluorophore entrapped in the bound Ab-tagged liposomes, the size homogeneity of liposome is extremely important for diagnostic applications. To reduce size heterogeneity, the liposome preparation was extruded 20 times through 0.4 and 0.2 μm polycarbonate filters. A mean diameter of 180 nm with a standard deviation of 3.4 nm was determined using a particle size analyzer (Brookhaven Instruments Corporation, Holtsville, NY, USA) (Table 1). For liposomes of this diameter, we were able to calculate that the average volume of a single liposome was 3.0×10^{-12} μL, and the entrapped volume (assuming a bilayer thickness of 4 nm) was 2.7×10^{-12} μL. By assuming the CF concentration inside the liposomes was equal to the original solution (10 mM) and by comparing the fluorescence of lysed liposomes to that of standard CF solutions, it was possible to calculate that there were approximately 7.1×10^{12} liposomes/mL, and that each liposome contained about 1.1×10^{5} molecules of CF. If the average surface area of the DPPC molecules was 7.1 nm^2, and that of cholesterol was 1.9 nm^2 (Ho et al., 2006; Szoka and Papahadjopoulos, 1978), we estimated that approximately 46 molecules of anti-mouse IgG were on the outer surface of each liposome, given that 0.89 mol% of maleimide-derivatized liposomes reacted successfully with SH-derivatized antibodies.

3.2. Optimization of PEI concentrations and the pH of the GA reaction

To achieve maximum immobilization of capture antibodies on the surface of the optical fiber, we conducted an optimization. The fiber was first coated with various concentrations of PEI (1%, 2%, 5%, and 10%), and then coated with anti-mouse IgG as the capture antibody to investigate the PEI effect on immobilizing the capture antibody by GA. Detailed experimental procedures were described previously in Section 2.5. Lysis of the bound liposome amplifiers released the CF dye, which enabled the measurement of the emitted fluorescence. As shown in Fig. 2A, the emitted fluorescence intensity was directly proportional to the concentration of PEI over a range of 1–5%, and it exhibited a maximum value at 5%. Furthermore, the difference in intensity of emitted fluorescence between the experimental (with the presence of target protein) and control (without the presence of target protein) groups was also directly proportional to the concentration of PEI (at a range of 1–5%). However, the emitted fluorescence intensity did not show any difference between the experimental and control groups when we used 10% PEI as a surface modifier. This indicated that although a high concentration of PEI results in a high surface concentration of immobilized capture antibody via GA, a steric effect may reduce significantly the binding efficiency of the capture antibody. In addition, a high concentration of PEI may also result in serious non-specific binding toward liposomal amplifiers. Considering all of these factors, we chose a concentration of PEI of 5% as optimum and used this concentration thereafter. The PEI-modified optical fiber was readily detected through XPS analysis. As shown in Fig. 2B and C, it exhibited signals at 398.4 eV and 399.7 eV, indicating the presence of N–H and O=C-N units at the surface, respectively, confirming the successful deposition of PEI on the surface of the optical fiber.

Furthermore, the structure of GA contains double-headed aldehyde groups and is commonly used as a homogeneous cross-linking reagent. Although the aldehyde groups are quite reactive, the environmental pH where the GA reaction took place significantly influences the reaction yield. Thus, in this study, FITC-labeled antibodies were utilized and coated on the surface of the plastic fibers using the PEI-GA modification procedure, where pH of the GA reaction mixture was set at 7.6, 9, and 10.5. Detailed procedures for this experiment were described previously in Section 2.5. And finally, unbound FITC-labeled antibody that remained in the solution was collected and measured with a fluorescence spectrophotometer to determine immobilization yield of antibody molecules. The weakest fluorescence of the solution was observed at pH of 9 or 10.5 (Fig. 3A), and the control group (no PEI-GA was modified on the optical fiber surface) exhibited the strongest fluorescence signal, meaning very few FITC-labeled antibody was modified onto the fiber surface. We thus concluded that, at pH 9 or 10.5, the highest GA reaction activity was achieved. Fig. 3B and C showed the fluorescence images of optical fibers modified with FITC-labeled antibodies at different conditions, consistent with the above, the highest immobilization of FITC-labeled antibodies was found at pH 9; we then selected pH of 9 as the most suitable reaction parameter and used that pH throughout the study.

Table 1
Characteristics of the liposomal amplifiers, anti-IgG-tagged, CF-entrapped liposomes.

Mean diameter (nm)	**180**
Volume of liposome (μL)	**3.0×10^{-12}**
Liposome concentration (liposomes/mL)	**7.1×10^{12}**
CF concentration (mM)	**10**
CF molecules per liposome	**1.1×10^{5}**
Antibody molecules on the liposome amplifier surface	**46**

3.3. Performance of the liposome-based TIRF-FOB

To develop a highly sensitive assay for protein detection, a liposome-based TIRF-FOB was established to measure our selected model protein, IgG. Different dilutions of the target protein in PBS solution (0 pg/mL, 1 pg/mL, 10 pg/mL, 100 pg/mL, 1 ng/mL, 10 ng/mL, 100 ng/mL, and 1 μg/mL) were injected into the reaction chamber to interact with the capture antibodies (anti-IgG antibody) on the optical fiber surface. We then injected 150 μL of liposome amplifiers that contained ca. 1.1×10^{12} liposome amplifiers into the reaction chamber, allowed these liposome amplifiers to interact with the bound-target protein, which then formed a sandwich immuno-complex. The dose–response relationship between the normalized fluorescence signal and the target protein concentration over a range of 0–1 μg/mL is shown in Fig. 4, where the error bars indicate 1 standard deviation for at least 3 repetitions. The normalized fluorescence signal on the *y*-axis in Fig. 4 is equal to the measured fluorescence intensity minus the background level for each measurement, which was then normalized by the background level. Thus, the unit of the normalized fluorescence signal can be expressed as an arbitrary unit (a.u.), which can be written as:

$$\text{normalized fluorescence signal} = \frac{\text{fluorescence intensity} - \text{background level}}{\text{backgroundlevel}}$$

A hyperbolic (or sigmoidal) response curve is seen commonly in many biochemical interactions (e.g., antigen–antibody interactions) (Chang et al., 2013; Ho et al., 2010). We defined the operational detection limit after adding 3 times the standard deviation of the control (free of IgG) from its average value (99.7%

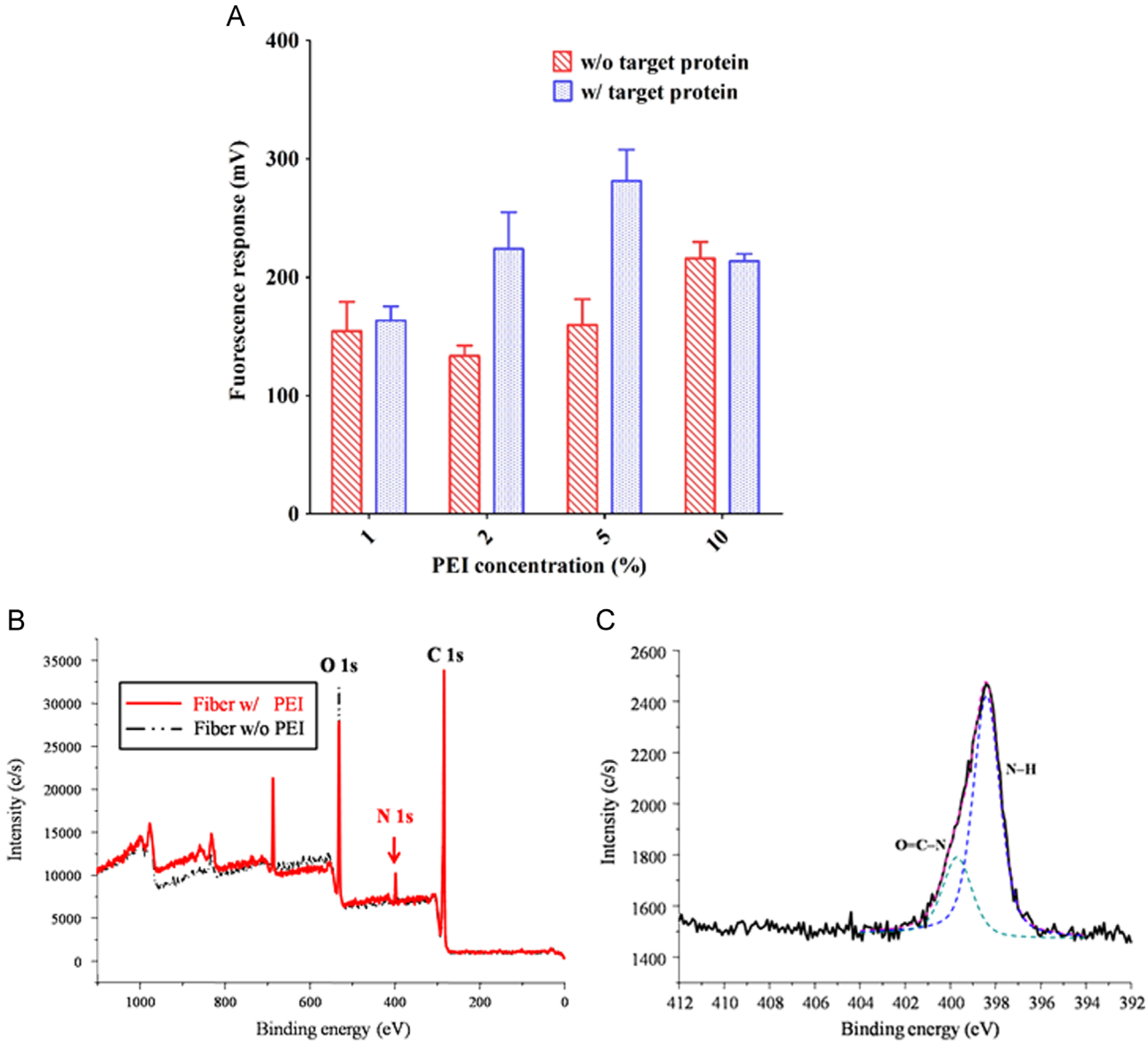

Fig. 2. (A) The emitted fluorescence response acquired by the TIRF-FOB was directly proportional to the concentration of PEI over a range of 1–5%, and it exhibited a maximum value at 5%; (B) X-ray photoelectron spectra of the surfaces of the PEI-coated optical fiber; (C) N1s XPS spectrum of the surfaces of the PEI-coated optical fiber.

confidence interval) based on the definition of International Union of Pure and Applied Chemistry (IUPAC). Accordingly, the LOD of our liposome-based TIRF-FOB was estimated to be 2.0 attomoles for the target protein (equivalent to 2.0 pg/mL of protein presented in 150 μL of sample solution), with a linear range of 10^2–10^5 pg /mL.

The ultrasensitive LOD of the liposome-based TIRF-FOB was ascribed to the following (i) the emitted fluorescence signal was intensified significantly, because each liposome contained more than 1×10^5 molecules of fluorophore, and all optical fiber-bound liposome amplifiers were able to be excited by evanescent waves; (ii) the emitted fluorescence signals were measured herein in the geometry that was normal to the reaction chamber, which resulted in a significant reduction in the background signal, in contrast to a conventional setup in which fluorescence was detected at the distal end of the optical fiber. In addition, with a conventional setup, the coaxial propagation of the pumping laser beam often induced a strong background signal, leading to a low LOD (Chang et al., 2010); (iii) fluorescence was excited herein using an intensity-modulated evanescent field, which could be measured precisely utilizing a very narrow bandwidth filter using a lock-in amplifier. Thus, in contrast to the conventional fluorescence detection methods, we anticipated an enhancement in the signal-to-noise ratio (Chao et al., 2012).

The advantages of the liposome-based TIRF-FOB system have been discussed previously; the disadvantages, however, included the lack of uniformity on the surface of ethyl acetate-treated optical fibers. This anomaly occurred in the de-cladding process in which the plastic optical fibers were stripped off their cladding by immersion in EA, resulting in uneven damage to the surface of the core. To compensate for such variations, we decided to normalize the data to reduce possible noise induced by variation in the optical fibers. Another strategy for improving the reproducibility of sensor performance is to utilize a tapered optical fiber where no further de-cladding is needed. Furthermore, the use of the tapered optical fiber allowed us to manipulate the magnitude of the evanescent field and the penetration depth thereby improving the LOD (Leung et al., 2007).

We believe that the liposome-based TIRF-FOB exhibited good biospecificity – the emitted fluorescence was acquired from

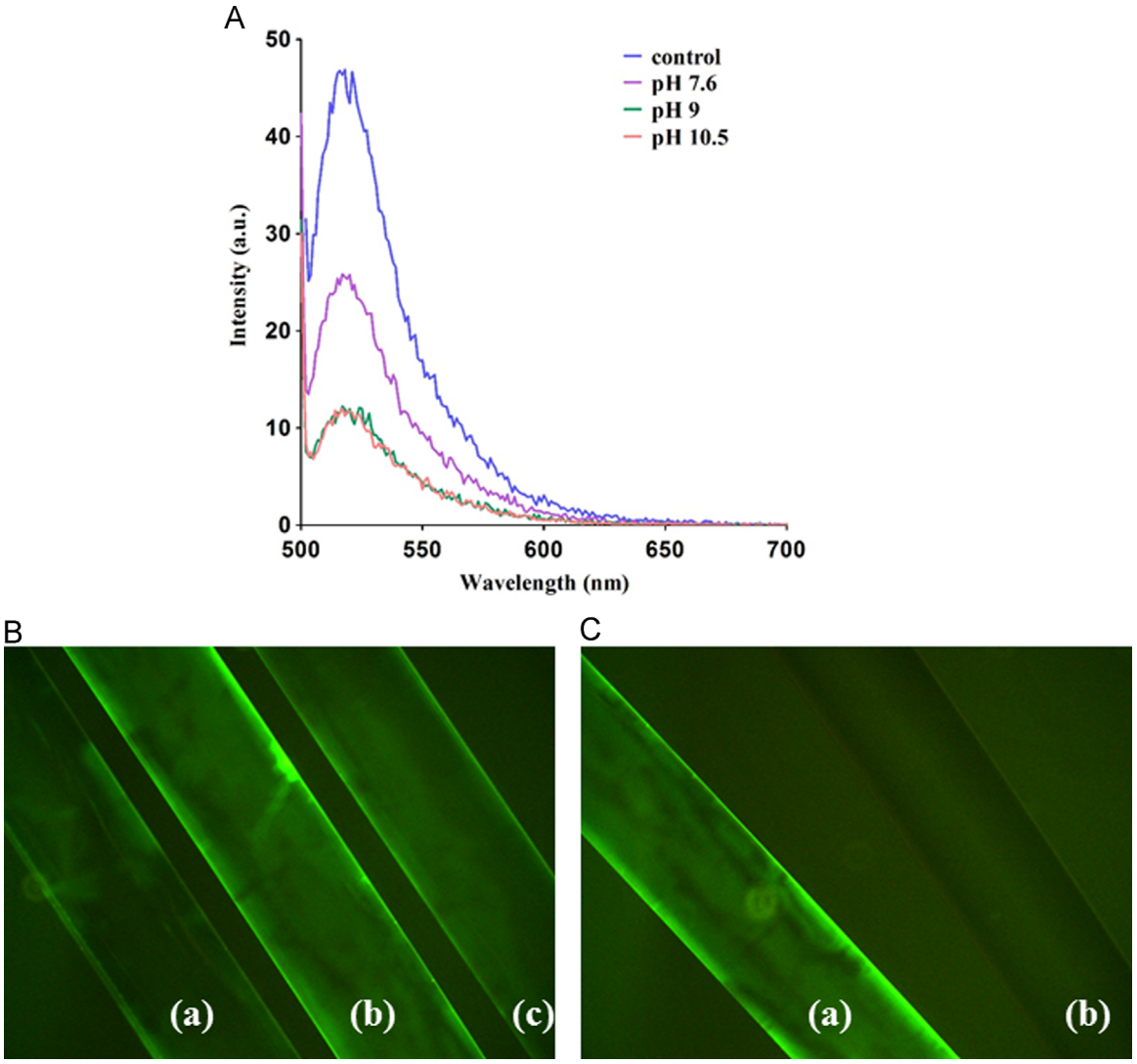

Fig. 3. (A) Fluorescence spectra for un-reacted FITC-labeled antibody remained in the reaction solution. Unbound FITC-labeled antibody was collected and measured using a fluorescence spectrophotometer, because the fluorescence signal should be inversely proportional to the GA reaction activity. The weakest fluorescence signal was seen at a pH of 9 or 10.5, meaning more FITC-labeled antibody was covalently modified to the surface of optical fibers; (B) image taken by Fluorescence Microscope, where (a), (b), and (c) represented PEI-modified optical fibers coated with FITC-label antibody via GA with reaction conditions at pH 10.5, 9, and 7.6, respectively. Fiber@pH9 seemed to have maximum coating of FITC-labeled antibody; (C) Image taken by Fluorescence Microscope, where (a) represented PEI-modified, and (b) showed non-PEI-modified optical fiber coated with FITC-label antibody. No observable amount of FITC-labeled antibody was coated at fiber (b).

detection of antibody-tagged, liposome amplifiers that formed tight sandwich immuno-complexes with the target protein and the capture antibody. This may be attributed to the inherited nature of the sandwich immunoassay format, because two antibodies (capture and detection antibodies) were used to capture specifically the model analyte. Moreover, the appropriate blocking strategy was adapted to prevent non-specific binding between the optical fiber surfaces and the target antibody molecules or liposomal amplifiers. To sum up, the specificity of the sandwich assay was generally higher than other immunoassays, such as the direct labeling, single-capture antibody format (Kingsmore, 2006). At a zero calibrator (without the presence of IgG), we added BSA (1 mg/mL) as a negative control; we found that the signal output was lower than other calibrators (with more than 1 pg/mL of IgG), which once again verified that our system offered high specificity and did not cross-react with other common proteins present in the sample.

4. Conclusions

To the best of our knowledge, a sensitive TIRF-FOB in combination with liposome amplifiers for protein detection was developed and demonstrated for the first time in this study. The use of 2 identical polyclonal antibodies in our assay development not only increased the specificity of the assay performance, but it also resulted in the cost-effectiveness of the sensor. Our newly-developed system is comparable to the conventional immunoassay with respect to the cost-performance ratio. Experimentally, our system was able to detect target protein (IgG) in PBS solution, and the LOD of the biosensor was calculated to be 2.0 attomoles for the target protein (equivalent to 2.0 pg/mL of protein presented in 150 μL of sample solution).

The improved sensitivity obtained here was achieved not only by the greater light intensity in the evanescent field as compared to that of transmitted light, but also through the contribution of the meticulously designed liposomal signal amplifier. In addition, the proposed biosensor could have great potential for multiplex

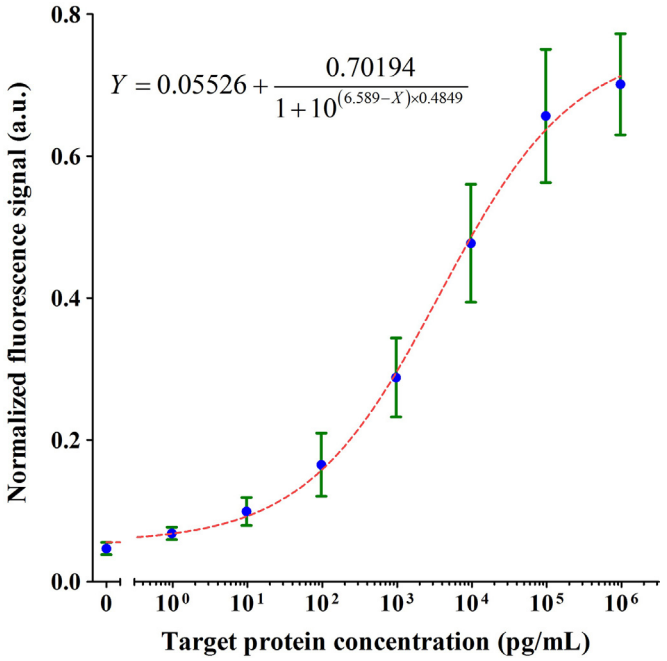

Fig. 4. The four-parameter dose-response relationship of a serially-diluted target protein in the PBS solution, as detected by the liposome-based TIRF-FOB over a concentration range of 1 pg/mL to 1 μg/mL. The data points and error bars represent the means and standard errors for the different concentration of target protein ($n \geq 3$).

detection, because it is possible for the optical fiber to guide light in different wavelengths simultaneously. Compared with other modern biosensors, our method offers multiple advantages, such as the simple structure of the optical setup, ease of operation, cost-effectiveness, high sensitivity, high specificity, and the possibility of multi-channel operation. Accordingly, our liposome-based TIRF-FOB could become a useful diagnostic tool to detect protein markers for cancer or other diseases.

Acknowledgments

This research was supported by the Taiwan Ministry of Science and Technolog, under grant Nos. 98-2627-B-007-001, 102-2628M-002-004-MY4 and 103-2811-M-002-163, and the Taiwan Ministry of Education "Aim for the Top University Plan" (EMRPD1A0751). Appreciation also goes to Chang Gung Memorial Hospital, research grant (CMRPD290092).

Appendix A. Supplementary material

Supplementary data associated with this article can be found in the online version at doi:http://dx.doi.org/10.1016/j.bios.2015.10.012.

References

Bangham, A.D., Standish, M.M., Weissmann, G., 1965. J. Mol. Biol. 13 (1), 253–259.
Chandrasekaran, S., King, M.R., 2014. Int. J. Mol. Sci. 15 (11), 20209–20239.
Chang, Y.-F., Hung, S.-H., Su, L.-C., Chen, R.-C., Chou, C., 2014a. Sens. Biosens. Res. 2, 1–7.
Chang, Y.F., Chao, C.H., Lin, L.Y., Tsai, C.H., Chou, C., Lee, Y.J., 2014b. J. Biomed. Opt. 19 (1), 011004.
Chang, Y.F., Chen, R.C., Lee, Y.J., Chao, S.C., Su, L.C., Li, Y.C., Chou, C., 2009. Biosens. Bioelectron. 24 (6), 1610–1614.
Chang, Y.F., Hung, S.H., Lee, Y.J., Chen, R.C., Su, L.C., Lai, C.S., Chou, C., 2011. Anal. Chem. 83 (13), 5324–5328.
Chang, Y.F., Tsao, K.C., Liu, Y.C., Chen, Y.C., Yu, P.C., Huang, Y.C., Chou, C., 2015. J. Virol. Methods 213, 151–156.
Chang, Y.F., Wang, S.F., Huang, J.C., Su, L.C., Yao, L., Li, Y.C., Wu, S.C., Chen, Y.M., Hsieh, J.P., Chou, C., 2010. Biosens. Bioelectron. 26 (3), 1068–1073.
Chang, Y.F., Yu, J.S., Chang, Y.T., Su, L.C., Wu, C.C., Chang, Y.S., Lai, C.S., Chou, C., 2013. Biosens. Bioelectron. 41, 232–237.
Chao, C.-H., Chang, Y.-F., Chen, H.-C., Lin, L.-Y., Yu, P.-C., Chang, Y.-S., Lee, Y.-J., Chou, C., 2012. Sens. Actuator B-Chem. 173, 184–190.
Chaudhery, V., George, S., Lu, M., Pokhriyal, A., Cunningham, B.T., 2013. Sensors 13 (5), 5561–5584.
Fan, N.-C., Cheng, F.-Y., Ho, J.-aA., Yeh, C.-S., 2012. Angew. Chem.-Int. Edit. 51 (35), 8806–8810.
Geng, J.L., Zhou, L., Liu, B., 2013. Chem. Commun. 49 (42), 4818–4820.
Hao, X.-j., Zhou, X.-h., Zhang, Y., Liu, L.-h., Long, F., Song, L., Shi, H-c, 2014. Sens. Actuator B-Chem 204, 682–687.
Ho, J.A., Fan, N.C., Jou, A.F., Wu, L.C., Sun, T.P., 2012. Talanta 99, 683–688.
Ho, J.A., Hsu, H.W., Huang, M.R., 2004. Anal. Biochem. 330 (2), 342–349.
Ho, J.A., Zeng, S.C., Huang, M.R., Kuo, H.Y., 2006. Anal. Chim. Acta. 556 (1), 127–132.
Ho, J.A.A., Chang, H.C., Shih, N.Y., Wu, L.C., Chang, Y.F., Chen, C.C., Chou, C., 2010. Anal. Chem. 82 (14), 5944–5950.
Ho, J.A.A., Hsu, H.W., 2003. Anal. Chem. 75 (16), 4330–4334.
Ho, J.A.A., Hung, C.H., 2008. Anal. Chem. 80 (16), 6405–6409.
Ho, J.A.A., Wu, L.C., Huang, M.R., Lin, Y.J., Baeumner, A.J., Durst, R.A., 2007. Anal. Chem. 79 (1), 246–250.
Ho, J.A.A., Zeng, S.C., Tseng, W.H., Lin, Y.J., Chen, C.H., 2008. Anal. Bioanal. Chem. 391 (2), 479–485.
Hsieh, B.Y., Chang, Y.F., Ng, M.Y., Liu, W.C., Lin, C.H., Wu, H.T., Chou, C., 2007. Anal. Chem. 79 (9), 3487–3493.
Huang, J.C., Chang, Y.F., Chen, K.H., Su, L.C., Lee, C.W., Chen, C.C., Chen, Y.M., Chou, C., 2009. Biosens. Bioelectron. 25 (2), 320–325.
Kingsmore, S.F., 2006. Nat. Rev. Drug. Discov. 5 (4), 310–320.
Kronick, M.N., Little, W.A., 1975. J. Immunol. Methods 8 (3), 235–240.
Lakowicz, J.R., Malicka, J., D'Auria, S., Gryczynski, I., 2003. Anal. Biochem. 320 (1), 13–20.
Leung, A., Shankar, P.M., Mutharasan, R., 2007. Sens. Actuator B-Chem. 125 (2), 688–703.
Liu, J., Lin, G., Xiao, C., Xue, Y., Yang, A., Ren, H., Lu, W., Zhao, H., Li, X., Yuan, Z., 2015a. Biosens. Bioelectron. 71, 82–87.
Liu, L.-h., Zhou, X.-h., Shi, H.-c., 2015b. Biosens. Bioelectron. 72, 300–305.
Marazuela, D., Moreno-Bondi, M.C., 2002. Anal. Bioanal. Chem. 372 (5–6), 664–682.
Niehage, C., Stange, C., Anitei, M., Hoflack, B., 2014. Liposome-based assays to study membrane-associated protein networks. In: Conn, P.M. (Ed.), Endosome Signaling, Pt A, pp. 223–243.
Noble, G.T., Stefanick, J.F., Ashley, J.D., Kiziltepe, T., Bilgicer, B., 2014. Trends Biotechnol 32 (1), 32–45.
Patil, Y.P., Jadhav, S., 2014. Chem. Phys. Lipids 177, 8–18.
Pokhriyal, A., Lu, M., Chaudhery, V., Huang, C.S., Schulz, S., Cunningham, B.T., 2010. Opt. Express 18 (24), 24793–24808.
Queiros, R.B., Gouveia, C., Fernandes, J.R.A., Jorge, F.A.S., 2014. Biosens. Bioelectron. 62, 227–233.
Su, L.C., Chang, Y.F., Chou, C., Ho, J.A., Li, Y.C., Chou, L.D., Lee, C.C., 2011. Anal. Chem. 83 (9), 3290–3296.
Szoka, F., Papahadjopoulos, D., 1978. Proc. Natl. Acad. Sci. USA 75 (9), 4194–4198.
Vamvakaki, V., Fournier, D., Chaniotakis, N.A., 2005. Biosens. Bioelectron. 21 (2), 384–388.
Wang, R., Xiang, Y., Zhou, X., Liu, L.-h, Shi, H., 2015. Biosens. Bioelectron. 66, 11–18.
Wang, X.D., Wolfbeis, O.S., 2013. Anal. Chem. 85 (2), 487–508.
Woodle, M.C., 1995. Adv. Drug Deliv. Rev. 16 (2–3), 249–265.
Yu, Y., Liu, Y., Zhen, S.J., Huang, C.Z., 2013. Chem. Commun. 49 (19), 1942–1944.
Zhang, S., Garcia-D'Angeli, A., Brennan, J.P., Huo, Q., 2014. Analyst 139 (2), 439–445.